Synthesis of Star-Shaped Poly(ε-caprolactone)-*b*-poly(L-lactide) Copolymers: From Star Architectures to Crystalline Morphologies

Jie Ren,[1,2] Zhonghai Zhang,[1] Yue Feng,[1] Jianbo Li,[1] Weizhong Yuan[1]

[1]*Institute of Nano- and Bio-polymeric Materials, School of Material Science and Engineering, Tongji University, Shanghai 200092, People's Republic of China*
[2]*Key laboratory Advanced Civil Engineering Materials, School of Material Science and Engineering, Ministry of Education, Tongji University, Shanghai 200092, People's Republic of China*

Received 29 December 2009; accepted 10 April 2010
DOI 10.1002/app.32590
Published online 29 June 2010 in Wiley InterScience (www.interscience.wiley.com).

ABSTRACT: Hexa-armed star-shaped poly(ε-caprolactone)-*block*-poly(L-lactide) (6sPCL-*b*-PLLA) with dipentaerythritol core were synthesized by a two-step ring-opening polymerization. GPC and ^{1}H NMR data demonstrate that the polymerization courses are under control. The molecular weight of 6sPCLs and 6sPCL-*b*-PLLAs increases with increasing molar ratio of monomer to initiator, and the molecular weight distribution is in the range of 1.03–1.10. The investigation of the melting and crystallization demonstrated that the values of crystallization temperature (T_c), melting temperature (T_m), and the degree of crystallinity (X_c) of PLLA blocks are increased with the chain length increase of PLLA in the 6sPCL-*b*-PLLA copolymers. On the contrary, the crystallization of PCL blocks dominates when the chain length of PLLA is too short. According to the results of polarized optical micrographs, both the spherulitic growth rate (G) and the spherulitic morphology are affected by the macromolecular architecture and the length of the block chains. © 2010 Wiley Periodicals, Inc. J Appl Polym Sci 118: 2650–2658, 2010

Key words: star-block copolymer; ring-opening polymerization; poly(L-lactide); crystallization; spherulites

INTRODUCTION

Poly(L-lactide) (PLLA) and PLLA-based blends and copolymers are the most innovative materials being actively investigated for their use in biomedical and packaging materials due to their biodegradability, biocompatibility, and producible from renewable resources.[1–7] However, besides its long degradation time PLLA is usually hard and brittle, which hinders its usage in medical applications like orthopedic and dental applications.[8,9] To overcome these disadvantages, many investigation have been made in the modification of the physical and mechanical properties of PLLA. Some modifications, such as the addition of plasticizers or surfactants/compatiblizer, are usually required to improve its original properties. One method is to blend PLLA with other polymers to improve the physical properties of PLLA.[10–13] However only moderate improvement in mechanical properties was achieved. The alterative method to modify the properties of PLLA is copolymerization with other monomers. PLLA copolymers have been synthesized, for example, diblock poly(lactide)-*b*-poly(ε-caprolactone) (PLA-*b*-PCL) and triblock PLA-*b*-PCL-*b*-PLA copolymers that have attracted considerable attention because of the combination of the good permeability of PCL with fast degradation of PLA segments.[14–16]

Another problem is related to the processing of PLLA.[17,18] Orthopedic applications of PLLA for fibers, bone plates, and screw require high-molecular weight PLLA, but molecular weight of PLLA tends to be lowered by degradation during processing at high temperature because of its high melt viscosity (for linear PLLA). There are several previous publications acknowledged this problem.[17–20] It was reported that branched (star-shaped) polymers could yield high-molecular-weight PLLA but with significantly lower melt viscosity than the linear PLLA.[21–24] Moreover, Star polymers have being gained great attention over the past decades due to their unique three-dimensional shape and properties. This has provoked considerable interest in the preparation of a variety of star copolymers with varying arm numbers, chemical composition, and chain topology.[25–32] For example, Tang and cowokers[33] reported synthesis and characterization of the star-shaped copolymer of PCL and PLLA from a cyclotriphosphazene core. Amass and coworkers[34] reported

Correspondence to: J. Ren (renjie6598@163.com).

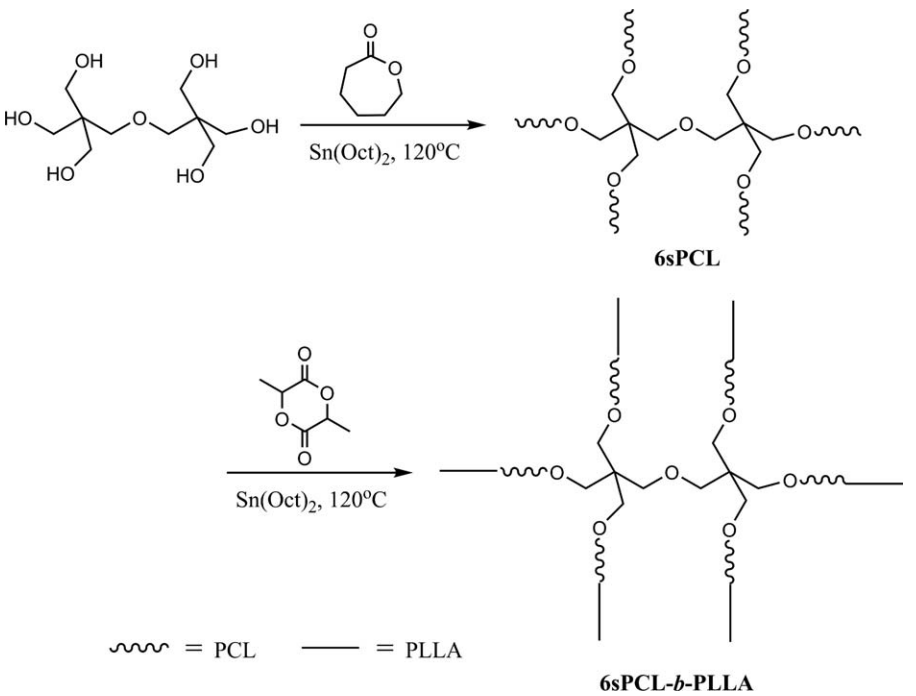

Scheme 1 Synthesis of the 6sPCL-*b*-PLLA star-block copolymers.

synthesis of 3-star-(PCL-*b*-PLA) block copolymers using potassium-based catalyst. And the effects of copolymer composition and molecular structure on the physical properties were investigated. Kim et al.[35] observed that star-shaped PLLA had a lower glass-transition temperature, melting temperature, and crystallinity than those of a linear analogue. Dong and coworkers reported the synthesis, crystallization behaviors of star-shaped PCLs, PLLAs, PCL-*b*-PEOs, and PLLA-*b*-PEOs with different numbers of arms.[36–42] Zhang[43] reported synthesis and characterization of dendritic star-shaped poly(epsilon-caprolactone)-*block*-poly(L-lactide) block copolymers. And the crystalline structure and thermal properties of the dendritic star-shaped polymers were investigated with X-ray diffraction and differential scanning calorimetry.

Star-shaped copolymers based on PCL and PLLA show very useful properties. However, studies on the effect of star-shaped architecture and chain composition on the crystallization and the spherulitic morphology of these star copolymers seem to be limited. In this article, we have synthesized a series of hexa-armed star-shaped PCL-*b*-PLLA copolymers with different chain length (Scheme 1). The thermal and crystallization behaviors of the hexa-armed PCL-*b*-PLLA star-block copolymers were investigated by differential scanning calorimetric analysis (DSC) and wide-angle X-ray diffraction (WAXD). The crystalline morphologies of the star-shaped copolymers were observed by polarized optical microscopy (POM).

EXPERIMENTAL

Materials

ε-Caprolactone (ε-CL; Acros Organic) was purified with CaH_2 by vacuum distillation. L-lactide (L-LA; TJL Biomaterials, Shanghai) was purified by twice recrystallization from ethyl acetate solution and dried in a vacuum at room temperature. Tin 2-ethylhexanoate ($Sn(Oct)_2$; Aldrich) was distilled under reduced pressure before use. Dipentaerythritol (Aldrich) was dried at 60°C *in vacuo* for 24 h before use. All other chemicals obtained from Sinopharm Chemical Regent Company (SCRC) were of analytical grade and were used as received.

Preparation of hydroxyl-terminated star-shaped poly(ε-caprolactone) (6sPCL)

The hydroxyl-terminated star-shaped poly(ε-caprolactone) (6sPCL) was synthesized by ring-opening polymerization of CL with dipentaerythritol as initiator. Briefly, CL (3.0 g, 26.3 mmol), dipentaerythritol (37.1 mg, 0.146 mmol) and a catalytic amount of $Sn(Oct)_2$ were added to a flame-dried polymerization tube quickly. The tube was then connected to a Schlenk line, where exhausting-refilling processes were repeated for three times. Then the tube was put into an oil bath at 120°C under nitrogen atmosphere with stirring and cooled to room temperature after polymerization for 24 h. The crude polymer was dissolved in chloroform and precipitated in cold methanol. The purified polymer was dried in a

vacuum oven at room temperature until constant weight.

Preparation of star-diblock copolymers (6sPCL-*b*-PLLA)

A typical polymerization procedure was as follows: The hydroxyl-terminated 6sPCL3 (2.404 g), L-LA (0.997 g, 6.925 mmol), and a dried magnetic stirring bar were added into a fire-dried polymerization tube quickly. The tube was then connected to a Schlenk line, where exhausting-refilling processes were repeated three times. The tube was put into an oil bath at 120°C with vigorous stirring for 5 min. A catalytic amount of $Sn(Oct)_2$ in anhydrous toluene was added to the melted mixture, and the exhausting-refilling process was carried out again to remove the toluene. The tube was put into an oil bath at 120°C under nitrogen atmosphere with stirring and cooled to room temperature after polymerization for 24 h. The resulting product was dissolved in chloroform and precipitated twice with methanol. The purified polymer was dried in a vacuum oven at room temperature until constant weight.

Characterization of 6sPCL and 6sPCL-*b*-PLLA

The structures of 6sPCL and 6sPCL-*b*-PLLA were characterized by FTIR and ^{1}H NMR. Attenuated total reflection Fourier transform infrared (ATR FTIR) spectra were recorded on an AVATAR 360 ESP FTIR spectrometer. ^{1}H NMR spectra were obtained using a Bruker DMX-500 NMR spectrometer with $CDCl_3$ as solvent at 25°C. The chemical shifts were relative to tetramethylsilane at $\delta = 0$ ppm for protons. The average molecular weight and its distribution were determined using a gel permeation chromatographic (GPC) system equipped with a Waters 150C separations module and a Waters differential refractometer. Polymer samples were dissolved in $CHCl_3$ at a concentration of 1–2 mg/ml. $CHCl_3$ was eluted at 1.0 mL/min through two Waters Styragel HT columns and a linear column. The internal and column temperatures were kept constant at 35°C.

Thermal analysis

DSC analysis was carried on a DSC-Q100 thermal analysis system (TA Instruments). Samples were first heated from 10 to 190°C at a heating rate of 10°C/min and held for 3 min to erase the thermal history, followed by cooling to −20°C at 10°C/min, and finally heated to 190°C at 10°C/min.

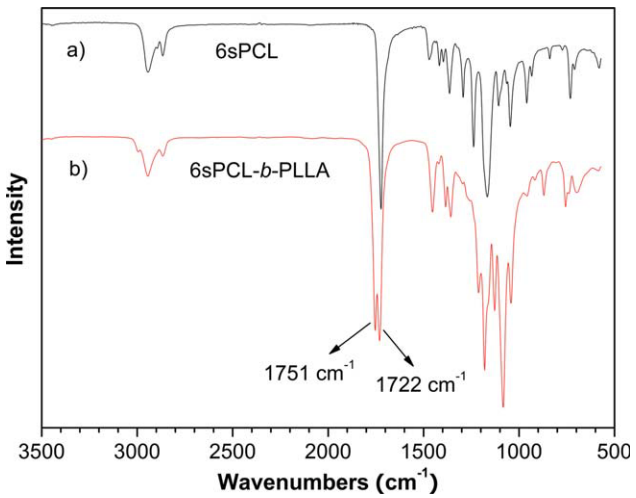

Figure 1 FTIR spectra of (a) 6sPCL3 and (b) 6sPCL-*b*-PLLA2. [Color figure can be viewed in the online issue, which is available at www.interscience.wiley.com.]

Crystalline analysis

WAXD patterns of film samples were obtained at room temperature on a Cu Kα radiation source using a D/max2550VB3+/PC X-ray diffractometer (Rigaku, Japan). The supplied voltage and current were set to 40 kv and 100 mA, respectively. Samples were exposed at a scanning rate $2\Theta = 4°$/min between 2Θ values from 3° to 50°. The crystalline morphology of the polymers was observed using a Leica DMLP polarized optical microscope (Leica Microsystems GmbH, Germany). Samples were prepared by spin-coating of polymer solution in chloroform (15 mg/ml) on a glass plate at room temperature and then were placed at room temperature for 24 h for complete evaporation of the solvent.

RESULTS AND DISCUSSION

Synthesis and characterization of star-shaped 6sPCLs and 6sPCL-*b*-PLLAs

Well-defined 6sPCL-*b*-PLLA copolymers were prepared via a two-step synthetic strategy. Firstly, 6sPCL was successfully synthesized via the controlled ring-opening polymerization of CL using dipentaerythritol as initiator, and $Sn(Oct)_2$ as catalyst (Scheme 1). Then these 6sPCLs with hydroxyl groups were used as macroinitiator for the following reaction with LLA.

The IR spectrum of the 6sPCL is shown in Figure 1(a). It can been clearly seen that the purified 6sPCL polymer shows the distinct stretching bands at 2943 cm^{-1} (characteristic of methylene group γ-CH) and 1722 cm^{-1} (C=O) for PCL. ^{1}H NMR spectrum of the star-shaped PCL is shown in Figure 2(a). It can be seen that the typical signals of the methylene protons of the dipentaerythritol initiator can be clearly

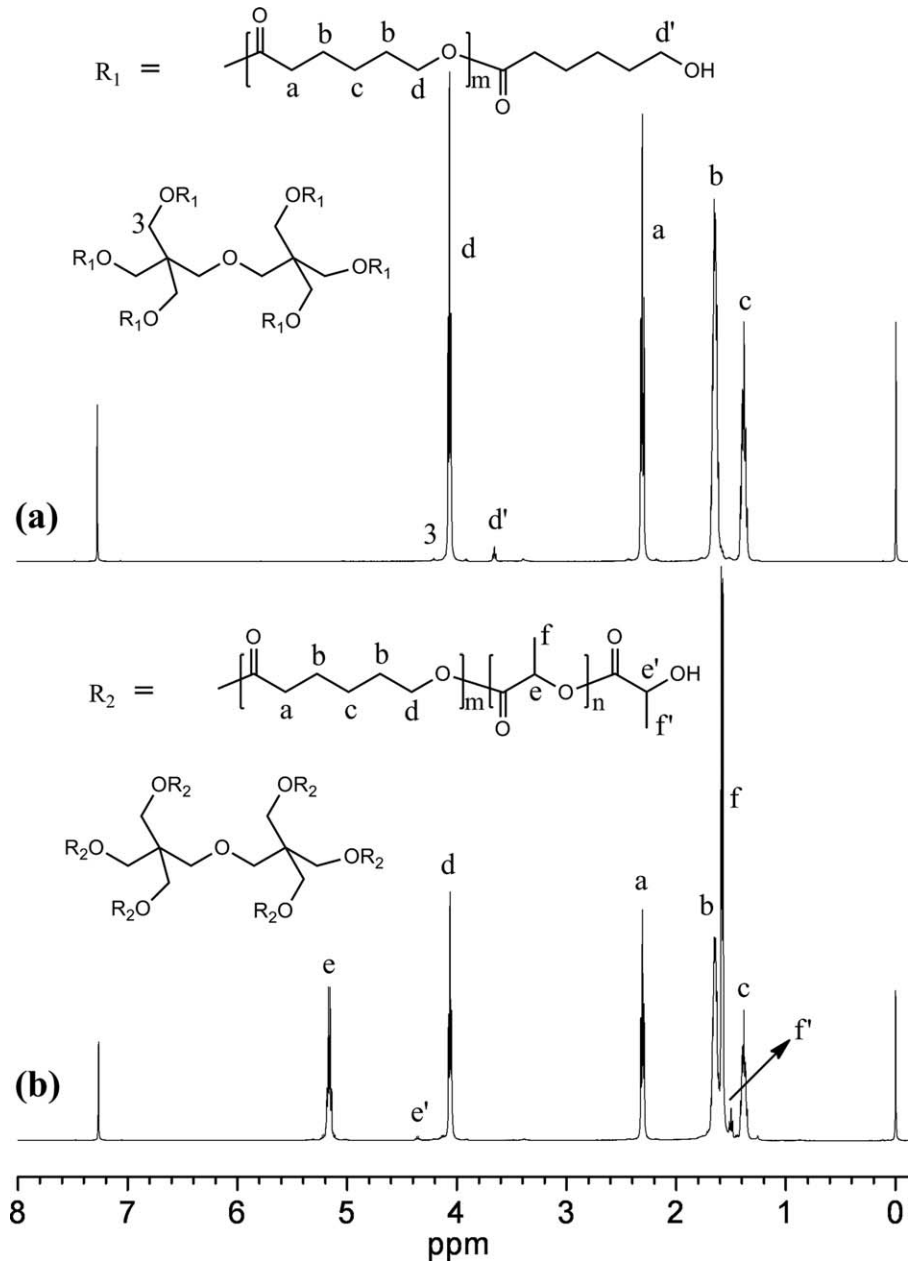

Figure 2 1H NMR spectrum of (a) 6sPCL3 and (b) 6sPCL-*b*-PLLA2.

detected at 4.19–4.24 ppm. The major resonance peaks (a–d) are attributed to PCL. The peak of the methylene (d) protons is detected at 4.06 ppm when the peak of the protons of the terminal methylene (d′) can be discovered at 3.65 ppm which indicates that PCL is terminated with hydroxyl groups. The average degrees of polymerization for the PCL arms can be calculated from the integration ratios between the methylene protons in the repeat units (d) and those in the terminal unit (d′) based on ^{1}H NMR spectrum. The molecular weight data of 6sPCL determined by ^{1}H NMR spectrum and GPC analysis are listed in Table I. The GPC traces of 6sPCL are shown in Figure 3. It can be seen that the traces are monomodal, which indicates that the sample is pure star-shaped PCL homopolymer. All these demonstrate that well-defined hexa-armed star-shaped PCLs with narrow number-average molecular weight distributions have been successfully synthesized by ring-opening polymerization (ROP) of CL with dipentaerythritol initiator.

FTIR is a useful tool to verify the presence of both PCL and PLLA components in purified star-shaped block copolymers. The IR spectrum of the 6sPCL-*b*-PLLA star-diblock copolymer is shown in Figure 1(b). The main difference in the IR spectrum between 6sPCL-*b*-PLLA and 6sPCL is the carbonyl absorption band region. In the IR spectrum of 6sPCL-*b*-PLLA, the

TABLE I
Synthesis of 6sPCL and 6sPCL-b-PLLA Star Copolymers by ROP[a]

Sample	[CL] : [LA] : [—OH]	$M_{n,th}$[b]	$M_{n,NMR}$[c]	$M_{n,GPC}$[d]	M_w/M_n[d]	Conversion (%)[e]
6sPCL1	10 : 0 : 1	6900	7900	10600	1.07	96.9
6sPCL2	20 : 0 : 1	13400	15500	17700	1.03	96.2
6sPCL3	30 : 0 : 1	19900	21000	27100	1.10	95.7
6sPCL3-b-PLLA1	30 : 10 : 1	28000	28100	33300	1.06	94.4
6sPCL3-b-PLLA2	30 : 30 : 1	43900	41600	47500	1.03	92.7
6sPCL3-b-PLLA3	30 : 50 : 1	59000	61400	62300	1.03	90.6

[a] Reaction conditions: [monomer]/[$Sn(Oct)_2$] = 1000, polymerization time = 24 h, polymerization temperature = 120°C.
[b] $M_{n,th}$ = [monomer]/[—OH] × 6 × $M_{monomer}$ × Conversion (%) + $M_{initiator}$; $M_{n,th}$ denotes the number-average molecular weight of star-shaped polymer.
[c] Determined by ^1H NMR spectroscopy of star-shaped polymer.
[d] Determined by GPC analysis with polystyrene standards.
[e] Conversion of monomer obtained from gravimetry.

carbonyl absorption band becomes wide and splits into two peaks. The peak at 1751 cm^{-1} corresponds to the carbonyl absorption of PLLA units, while the peak at 1722 cm^{-1} is assigned to the carbonyl absorption of PCL units. It is important to prove that the PLLA chains exist in the copolymer as a block. The ^1H NMR spectrum of 6sPCL-*b*-PLLA is shown in Figure 2(b). The peak assigned to the methylene protons of the PCL block at 3.65 ppm disappears, and two new peaks at 4.36 ppm (e′) and 1.50 ppm (f′) for the produced end groups of the PLLA blocks are observed. These indicate that the terminal hydroxyl groups of the 6sPCL macroinitiator successfully initiates the polymerization of L-LA. The average polymerization degree of L-LA is also determined by the integration ratio of methine protons of the PLLA block at 4.36 ppm and the methylene protons of PCL at 2.31 ppm. As shown in Table I, the number-average molecular weight of the resulting copolymers increases with increasing molar ratio of monomer to macroinitiator, which indicates that the hydroxyl-terminated star-shaped polyester can be used as effective propagation centers and all of the six hydroxyl groups of the star-shaped polyester molecule can initiate the ROP of L-LA. In addition, the molecular weight distributions of these polymers were narrow ($1.03 \leq M_w/M_n \leq 1.10$). The GPC traces of the star-diblock copolymer 6sPCL-*b*-PLLAs are shown in Figure 3. These traces are comparatively symmetrical and monomodal, suggesting that these purified polymers are pure homopolymer or star-block copolymers. As the note, $M_{n,GPC}$ has a little variation compared with both $M_{n,th}$ and $M_{n,NMR}$, which is from the star architecture of the polymer, and GPC is a relative method.

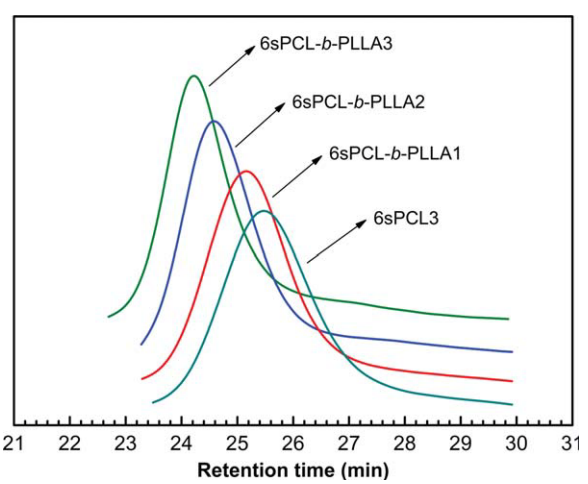

Figure 3 GPC traces of the 6sPCL and 6sPCL-*b*-PLLA copolymers. [Color figure can be viewed in the online issue, which is available at www.interscience.wiley.com.]

Differential scanning calorimetry and wide-angle X-ray diffraction analysis

The melting and crystallization behaviors of 6sPCL and 6sPCL-*b*-PLLA block copolymers were investigated by DSC as shown in Figure 4 and Table II.

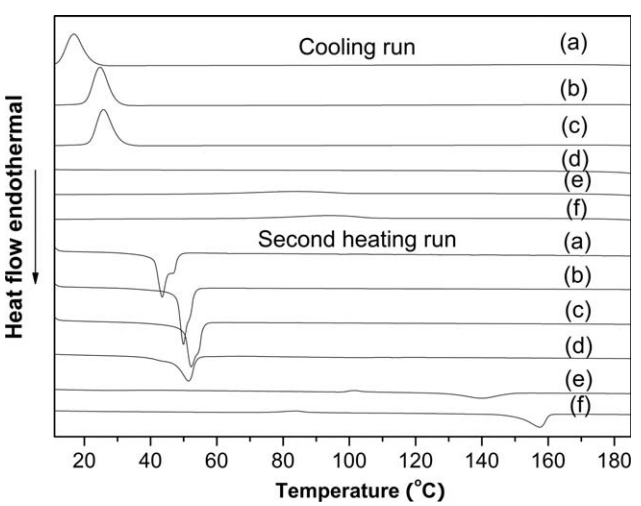

Figure 4 DSC curves of (a) 6sPCL1, (b) 6sPCL2, (c) 6sPCL3, (d) 6sPCL-*b*-PLLA1, (e) 6sPCL-*b*-PLLA2, and (f) 6sPCL-*b*-PLLA3 in the cooling run and second heating run, respectively.

TABLE II
Melting and Crystallization Behaviors of 6sPCL and 6sPCL-*b*-PLLA Block Copolymers

Sample	T_c (°C)[a]		T_m (°C)[b]		ΔH_m (J/g)[c]		X_c (%)[d]	
	$T_{c,PCL}$	$T_{c,PLLA}$	$T_{m,PCL}$	$T_{m,PLLA}$	$\Delta H_{m,PCL}$	$\Delta H_{m,PLLA}$	$X_{c,PCL}$	$X_{c,PLLA}$
6sPCL1	22.04		41.04		69.62		51.15	
6sPCL2	29.44		47.91		68.99		50.69	
6sPCL3	30.74		50.15		67.08		49.29	
6sPCL-*b*-PLLA1	11.51		46.56		48.18		35.40	
6sPCL-*b*-PLLA2		99.79		129.68		22.35		23.88
6sPCL-*b*-PLLA3		106.84		150.36		30.20		32.26

[a] $T_{c,PCL}$ and $T_{c,PLLA}$ denote the crystallization temperatures of PCL and PLLA segments in the cooling run, respectively.
[b] $T_{m,PCL}$ and $T_{m,PLLA}$ are the melting points of PCL and PLLA segments in the second heating run, respectively.
[c] $\Delta H_{m,PCL}$ and $\Delta H_{m,PLLA}$ denote the fusion enthalpies of PCL and PLLA segments in the second heating run, respectively.
[d] $X_{c,PCL} = \Delta H_{m,PCL}/\Delta H^0_{m,PCL}$ and $X_{c,PLLA} = \Delta H_{m,PLLA}/\Delta H^0_{m,PLLA}$, where $\Delta H^0_{m,PCL}$ is 136.1 J/g and $\Delta H^0_{m,PLLA}$ is 93.6 J/g.

The crystallization temperature (T_c) was obtained from the cooling run, and the melting temperature (T_m) and the degree of crystallinity (X_c) were obtained from the second heating run. The results listed in Table II show that T_c and T_m of 6sPCLs increase with the length increase of the PCL arms, which are attributed mainly to the crystalline imperfection of the short chain length of PCL segments in the star-shaped polymers. Meanwhile, the star-shaped structure of these copolymers should make a contribution to the imperfection. It should be noted that X_c of 6sPCLs does not increase with the length increase of the PCL arms but remains nearly constant ($X_c = \sim 50\%$). This indicates that the contribution of chain length to the degree of crystallinity of star-shaped polymers is limited when the length of the PCL arms is long enough, which is in good agreement with the results reported by Wang et al.[36]

From the DSC curves shown in Figure 4, a weak T_c peak of PCL blocks can been seen in the cooling run and a weak T_m peak in the second heating run within 6sPCL-*b*-PLLA1 block copolymer, and the values are obviously lower than that of PCL in its precursor, 6sPCL3. This can be attributed to the restriction of the outer PLLA block to the inner PCL block. Furthermore, the T_c and T_m peaks of PLLA block does not appear in the DSC curves of 6sPCL-*b*-PLLA1, which is mainly attributed to the shorter arm length of PLLA linking to the PCL core., It can be seen that with increasing length of PLLA arms the T_c and T_m peaks of PLLA appear while that of PCL disappear in the DSC curves of 6sPCL-*b*-PLLA2 and 6sPCL-*b*-PLLA3 copolymers. This is attributed to the fact that the macromolecular mobility of inner PCL blocks is spatially restricted by the outer PLLA block, and the crystallization of PLLA block nearly hampers completely that of PCL block. In the other hand, the T_c and T_m values of PLLA in 6sPCL-*b*-PLLA copolymers increase from 99.79 and 129.68°C to 106.84 and 150.36°C, while the degree of crystallinity of that also is enhanced with the increasing length of PLLA blocks. All these indicate that the values of T_c, T_m, and X_c are affected by the length of the block chains.

WAXD is another useful method to demonstrate the crystal structure of these star-shaped block copolymers in solid-state. Figure 5 shows WAXD patterns of star-shaped 6sPCL3 and 6sPCL-*b*-PLLA copolymers.

It is well known that linear PCL shows intensive peaks at about 21.6° and 23.9°, corresponding to the (110) and (200) planes of the orthorhombic crystal form,[44,45] while purified PLLA presents prominent diffraction peaks at about 16.5° and 19° that are characteristic of the PLLA crystal.[46] From Figure 5, it can be seen that 6sPCL displays the same crystalline structure as linear PCL. WAXD pattern of 6sPCL-*b*-PLLA1 has two peaks at 21.4° and 23.3° for the PCL segments in the copolymer, and the other two weak

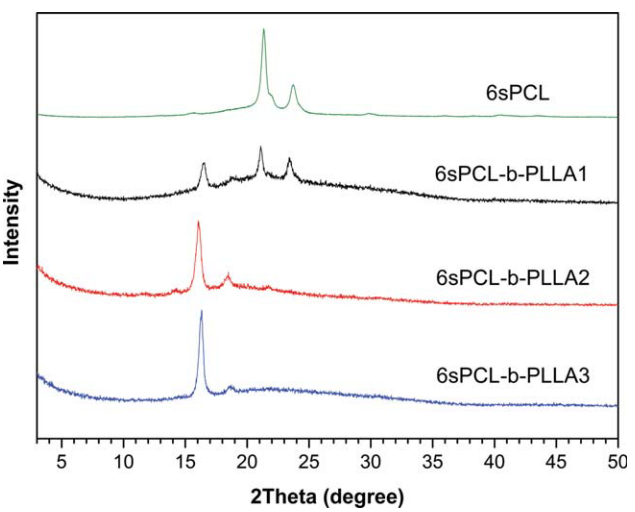

Figure 5 WAXD patterns of 6sPCL, 6sPCL-*b*-PLLA1, 6sPCL-*b*-PLLA2, and 6sPCL-*b*-PLLA3 copolymer. [Color figure can be viewed in the online issue, which is available at www.interscience.wiley.com.]

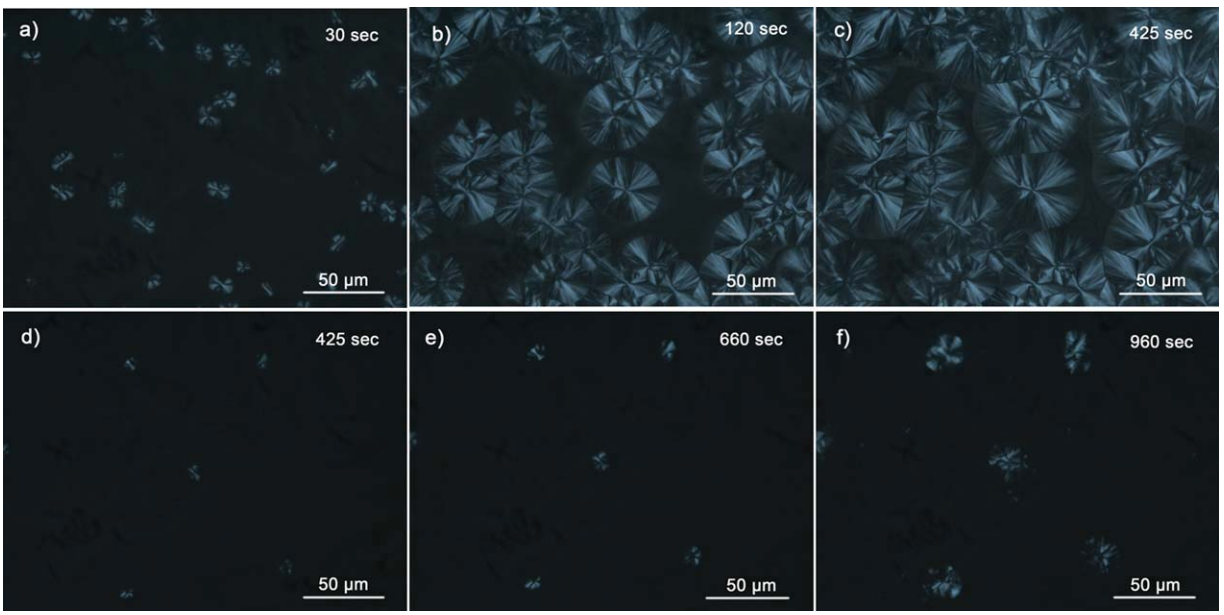

Figure 6 The polarized optical micrographs of the isothermal crystallization of both 6sPCL (A–C; scale bar: 50 μm) and 6sPCL-*b*-PLLA1 (D,E; scale bar: 50 μm) at a crystallization temperature of 38°C. [Color figure can be viewed in the online issue, which is available at www.interscience.wiley.com.]

peaks at 16.2° and 18.7° for PLLA block. However, only the diffraction peaks of PLLA crystal at 16.2° and 18.7° can be detected for 6sPCL-*b*-PLLA2 and 6sPCL-*b*-PLLA3, which indicates that the PCL chains present as amorphous. This result agrees with the earlier DSC analysis.

Crystalline morphologies of star-shaped polymers

The crystalline morphology and the spherulitic growth process of 6sPCL3 and 6sPLA-*b*-PLLAs were investigated by POM. The isothermal crystallization temperature was chosen between T_m and T_c of the block.[37] According to the earlier DSC analysis, it is known that only the T_c of PCL blocks in the 6sPCL-*b*-PLLA1 block copolymer and only the T_c of PLLA block in the star-shaped 6sPCL-*b*-PLLA2 and 6sPCL-*b*-PLLA3 block copolymers can be clearly observed. So 38°C was chosen as the isothermal crystallization temperature of 6sPCL3 and 6sPCL-*b*-PLLA1 while 120°C was chosen as that of 6sPCL-*b*-PLLA2 and 6sPCL-*b*-PLLA3. From Figure 6(A–C), we can see that the crystals of 6sPCL3 show a typical spherulitic morphology. As for 6sPCL-*b*-PLLA1 copolymer, the size of the spherulites is much smaller than that of 6sPCL, and no clear Maltese cross patterns are discovered. The results can be attributed to the star-shaped structure of copolymer and the presence of PLLA block in the copolymer interfering with the natural growth of the spherulitic. The spherulitic growth rate of 6sPCL-*b*-PLLA3 is apparently higher than that of 6sPCL-*b*-PLLA2 from the Figure 7. This indicates that the spherulitic growth rate of 6sPCL-*b*-PLLA increases slightly with increasing length of PLLA block. The average spherulitic diameter was then plotted against the isothermal crystallization time as shown in Figure 8. The spherulitic diameter increases linearly with the isothermal crystallization time, and the spherulitic growth rate (G) can be evaluated from the slope of theses lines. From Figure 8, it can be seen that the spherulitic growth rate of PCL block in 6sPCL3 is apparently higher than that in 6sPCL-*b*-PLLA1, and G of PLLA block in 6sPCL-*b*-PLLA3 is higher than that in 6sPCL-*b*-PLLA2. These indicate that both G and the spherulitic morphology are affected by the macromolecular architecture and the length of the block chains.

CONCLUSION

Hexa-armed star-shaped block copolymers based on biodegradable and crystalline PCL and PLLA were synthesized successfully via a two-step ring-opening polymerization. 6sPCL was prepared by ROP using dipentaerythritol as initiator, and then it was used as macroinitiator for ROP of LLA to obtain 6sPCL-*b*-PLLA copolymers. The results of DSC analysis show that T_c and T_m of 6sPCLs increase with the length increase of the PCL arms while that of PLLA in the 6sPCL-*b*-PLLA copolymers are also increase by increasing length of the outer PLLA blocks, which is attributed to the crystalline imperfection of the short chain length and the contribution of the star-shaped structure to the imperfection. In addition, X_c of 6sPCLs does not increase with the length increase of the PCL arms but remains nearly constant (X_c =

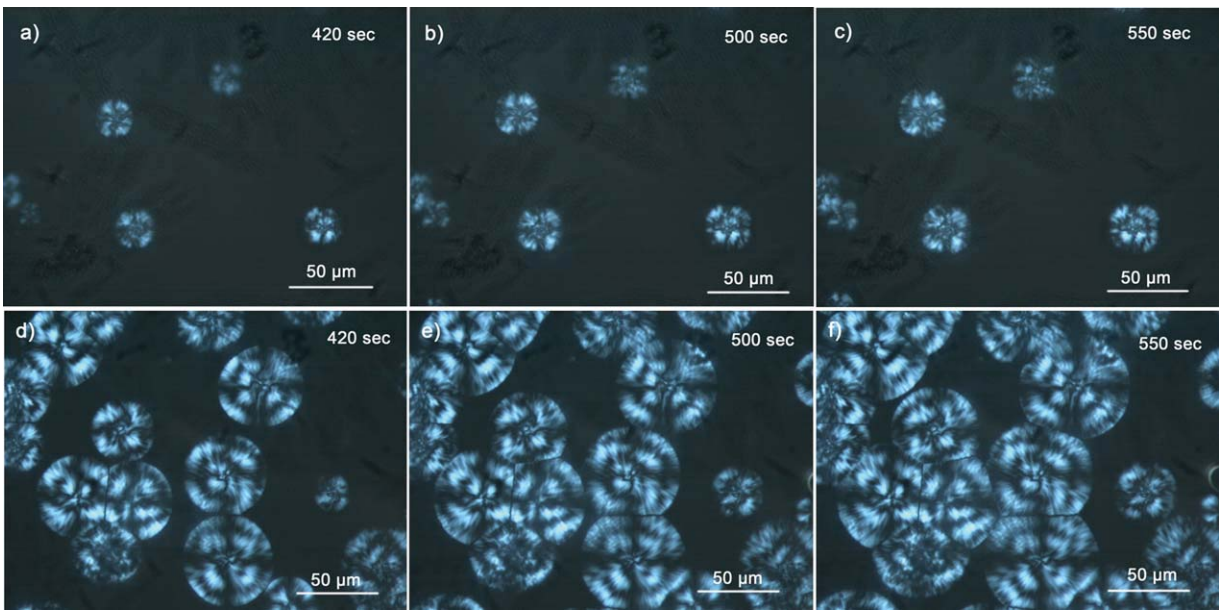

Figure 7 The polarized optical micrographs of the isothermal crystallization of both 6sPCL-*b*-PLLA2 (A–C; scale bar: 50 μm) and 6sPCL-*b*-PLLA3 (D,E; scale bar: 50 μm) at a crystallization temperature of 120°C. [Color figure can be viewed in the online issue, which is available at www.interscience.wiley.com.]

~ 50%). But in the 6sPCL-*b*-PLLA copolymers, the macromolecular mobility of the inner PCL block is restricted by the outer crystallized PLLA so that the degree of crystallinity of PCL block becomes lower and even an amorphous phase is formed. Moreover, the degree of crystallinity of PLLA in 6sPCL-*b*-PLLA copolymers increases with increasing length of outer PLLA blocks. The crystalline morphology and the spherulitic growth process of 6sPCL3 and 6sPLA-*b*-PLLAs were investigated by POM. These indicate that both the spherulitic growth rate (G) and the spherulitic morphology are affected by the macromolecular architecture and the length of the block chains.

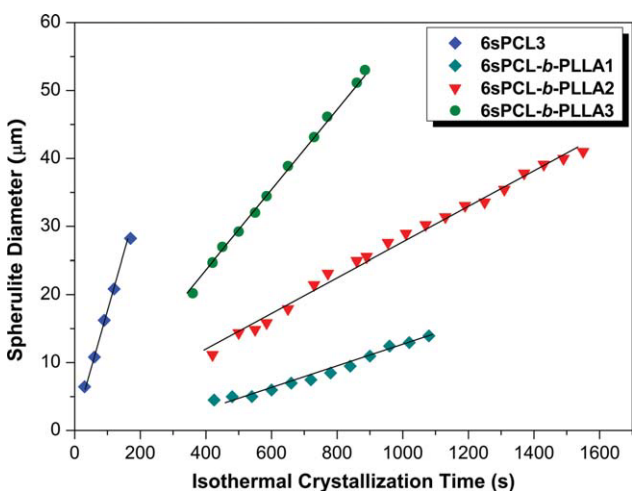

Figure 8 Dependence of the spherulite diameter on the isothermal crystallization time for PCL chains in 6sPCL3 and 6sPCL-*b*-PLLA1 at 38°C, and PLLA chains in 6sPCL-*b*-PLLA2 and 6sPCL-*b*-PLLA3 at 120°C. [Color figure can be viewed in the online issue, which is available at www.interscience.wiley.com.]

The authors gratefully acknowledge the financial support from the Program of Shanghai Subject Chief Scientist (No. 07XD14029) and the National Natural Science Foundation of China (No. 20804029).

References

1. Chen, C.; Lv, G.; Pan, C.; Song, M.; Wu, C. H.; Guo, D. D. Biomed Mater 2007, 2, L1.
2. Albertsson, A. C.; Varma, I. K. Biomacromolecules 2003, 4, 1466.
3. Jiao, Y. P.; Cui, F. Z. Biomed Mater 2007, 2, R24.
4. Mills, C. A.; Navarro, M.; Engel, E.; Martinez, E.; Ginebra, M. P.; Planell, J. J Biomed Mater Res Part A 2007, 67, 781.
5. Tai, H. Y.; Mather, M. L.; Howard, D.; Wang, W. X.; White, L. J.; Growe, J. A. Eur Cells Mater 2007, 14, 64.
6. Dechy-Cabaret, O.; Martin-Vaca, B.; Bourissou, D. Chem Rev 2004, 104, 6147.
7. Chen, H.; Peng, C. R.; Yao, Y. Y.; Wang, J. X.; Chen, Z. P.; Yang, Z. R.; Xia, L. J.; Liu, S. Y. J Appl Polym Sci 2009, 114, 3152.
8. Matsusue, Y.; Nakamura, T.; Iida, H.; Shimizu, K. J Long Term Eff Med Implants 1997, 7, 119.
9. Bergsma, J. E.; De Bruijn, W. C.; Rozema, F. R.; Bos, R. R. M.; Boering, G. Biomaterials 1995, 16, 25.
10. Hu, Y.; Rogunova, M.; Topolkaraev, V.; Hiltner, A.; Baer, E. Polymer 2003, 44, 5701.
11. Liu, X.; Dever, M.; Fair, N.; Benson, R. S. J Environ Polym Degrad 1997, 5, 225.
12. Jia, Z. Y.; Zhang, K. Y.; Tan, J. J.; Han, C. Y.; Dong, L. S.; Yang, Y. M. J Appl Polym Sci 2009, 111, 1530.
13. Tsuji, H. Polymer 2000, 41, 3621.
14. Huang, M. H.; Coudane, J.; Li, S. M.; Vert, M. J Polym Sci: Polym Chem 2005, 43, 4196.

15. Zhao, Z. X.; Yang, L.; Hu, Y. F.; He, Y.; Wei, J.; Li, S. M. Polym Degrad Stab 2007, 92, 1769.
16. Qian, H. T.; Bei, J. Z.; Wang, S. G. Polym Degrad Stab 2000, 68, 423.
17. Kim, S. H.; Han, Y. K.; Ahn, K. D.; Kim, Y. H.; Chang, T. Makromol Chem 1993, 194, 3229.
18. Tsuji, H.; Horikawa, G.; Itsuno, S. J Appl Polym Sci 2007, 104, 831.
19. Kim, S. H.; Han, Y. K.; Kim, Y. H.; Hong, S. Makromol Chem 1992, 193, 1623.
20. Grijpma, D. W.; Joziasse, C. A. P.; Pennings, A. J. Makromol Chem 1993, 14, 155.
21. Grijpma, D. W.; Pennings, A. J. Macromol Chem Phys 1994, 195, 1633.
22. Grijpma, D. W.; Pennings, A. J. Macromol Chem Phys 1994, 195, 1649.
23. Aragade, A. B.; Peppas, N. A. Polym Bull 1993, 31, 401.
24. Zhu, K. J.; Bihai, S.; Shilin, Y. J. Polym Sci Polym Chem Ed 1982, 20, 319.
25. Voit, B. J Polym Sci Part A: Polym Chem 2000, 38, 2505.
26. Ihre, H.; Padilla De Jesus, O. L.; Frchet, J. M. J. J Am Chem Soc 2001, 123, 5908.
27. Mckee, M. G.; Wilkes, G. L.; Long, T. E. Prog Polym Sci 2005, 30, 507.
28. Tomalia, D. A. Prog Polym Sci 2005, 30, 294.
29. Biela, T.; Duda, A.; Penczek, S.; Rode, K.; Pasch, H. Polym Sci Part A: Polym Chem 2002, 40, 2884.
30. Biela, T.; Duda, A.; Rode, K.; Pasch, H. Polymer 2003, 44, 1851.
31. Rao, J. Y.; Zhang, Y. F.; Zhang, J. Y.; Liu, S. Y. Biomacromolecules 2008, 9, 2586.
32. Li, J. B.; Ren, J.; Cao, Y.; Yuan, W. Z. Polymer 2010, 51, 1301.
33. Cui, Y. J.; Tang, X. Z.; Huang, X. B.; Chen, Y. Biomacromolecules 2003, 4, 1491.
34. Lemmouchi, Y.; Perry, M. C.; Amass, A. J.; Chakraborty, K.; Schacht, E. J Polym Sci Part A: Polym Chem 2008, 46, 5363.
35. Kim, E. S.; Kim, B. C.; Kim, S. H. J Polym Sci Part B: Polym Phys 2004, 42, 939.
36. Wang, J. L.; Wang, L.; Dong, C. M. J Polym Sci Part A: Polym Chem 2005, 43, 5449.
37. Wang, J. L.; Dong, C. M. Polymer 2006, 47, 3218.
38. Wang, L.; Cai, C.; Dong, C. M. Chin J Polym Sci 2008, 26, 161.
39. Wang, L.; Dong, C. M. J Polym Sci Part A: Polym Chem 2006, 44, 2226.
40. Hua, C.; Dong, C. M. J Biomed Mater Res Part A 2007, 82, 689.
41. Cai, C.; Wang, L.; Dong, C. M. J Polym Sci Part A:Polym Chem 2006, 44, 2034.
42. Liu, Q.; Cai, C.; Dong, C. M. J Biomed Mater Res Part A 2009, 88, 990.
43. Zhang, W.; Zheng, S.; Guo, Q. J Appl Polym Sci 2007, 106, 417.
44. Wang, L.; Wang, J. L.; Dong, C. M. J Polym Sci Part A: Polym Chem 2005, 43, 4721.
45. Chen, L.; Ni, Y. S.; Bian, X. C.; Qiu, X. Y.; Zhuang, X. L. Carbohydr Polym 2005, 60, 103.
46. Ikada, Y.; Jamshidi, K.; Tsuji, H.; Hyon, S. H. Macromolecules 1987, 20, 904.